applied sciences

MDPI

Article

Analytical Model for Contaminant Transport in the CGCW and Aquifer Dual-Domain System Considering GMB Holes

Long Ran [1,2], Guijun Wan [3], Hao Ding [3,*] and Haijian Xie [3]

[1] School of Civil Engineering and Architecture, Zhejiang University of Science and Technology, Hangzhou 310023, China; 122016@zust.edu.cn
[2] Zhejiang-Singapore Joint Laboratory for Urban Renewal and Future City, Hangzhou 310023, China
[3] The Architectural Design and Research Institute of Zhejiang University Co., Ltd., 148 Tianmushan Rd., Hangzhou 310058, China; wangj544731@126.com (G.W.); xiehaijian@zju.edu.cn (H.X.)
* Correspondence: hao.ding@zju.edu.cn

Abstract: Composite geomembrane cut-off walls (CGCW) have been widely used for the remediation of polluted sites, especially where the environmental conditions are complex. Accurate predictions of the GMB hole leakage and CGCW performance are essential for engineering design and cost control. This paper establishes empirical equations to predict the leakages through the CGCWs based on the numerical models. Additionally, an analytical solution for contaminant migration through the CGCW is proposed considering the effects of GMB holes. The accuracy of the established equations and analytical solution is verified by the numerical models. The key effects of the GMB thickness (T_G), head loss (H_G), cut-off wall hydraulic conductivity (k_G), hole radius (r_G) and shape on the leakage and CGCW performance are investigated. The results show that compared with other hole shapes, the leakage through the circular hole is lowest. This is mainly because the shape factor for the circular hole is 1.15–1.3 times lower than that for other shapes of holes with the same area. Additionally, the effects of the hole geometric properties and head loss on the CGCW performance can be more significant when the cut-off wall hydraulic coefficient is small. For example, the breakthrough time differences between the cases with r_G = 0.005 m and 0.05 m are 0.8 and 5.0 years when $k_G = 10^{-10}$ and 10^{-9} m/s, respectively. This is because the impermeability of the CGCW is good when k_G is small. This will weaken the impacts of the hole geometric properties on the leakage. The proposed empirical equations and analytical solution can provide effective suggestions for the design of the CGCW in different GMB hole cases.

Keywords: empirical equations; analytical solution; GMB holes; composite geomembrane cut-off wall

Citation: Ran, L.; Wan, G.; Ding, H.; Xie, H. Analytical Model for Contaminant Transport in the CGCW and Aquifer Dual-Domain System Considering GMB Holes. *Appl. Sci.* **2024**, *14*, 10280. https://doi.org/10.3390/app142210280

Academic Editor: Jaecheul Yu

Received: 24 September 2024
Revised: 28 October 2024
Accepted: 1 November 2024
Published: 8 November 2024

1. Introduction

Groundwater pollution caused by industrial sewage, pesticides and waste has become a worldwide concern [1,2]. The cut-off wall made of soil-bentonite (SB), cemented bentonite (CB), or soil-bentonite-cement (SBC) is widely to prevent groundwater from being polluted by contaminants [3,4]. However, the performance of SB, CB, or SBC can be easily influenced by extreme or complex conditions such as wet-dry cycles and freeze-thaw cycles [5]. This will lead to an increase in the hydraulic conductivity of the cut-off wall [6,7]. It has been reported that the composite geomembrane cut-off walls (CGCWs) with low permeability and high chemical resistance geomembranes (GMBs) embedded can effectively solve this problem [8,9]. This type of barrier has been widely used for the remediation of polluted sites, especially where the environmental conditions are complex [10].

Accurate predictions of the CGCW performance are essential for engineering design and cost control [11]. Experiments, numerical simulations and analytical solutions are the primary tools to analyze the contaminant migration process and predict the service times of the CGCWs [12,13]. For example, Wang et al. [14] compared the transport behaviors of different types of contaminants in the CGCWs. Xu et al. [13] conducted the permeability

test to evaluate the hydraulic performance of the CGCWs based on the flexible wall permeameter. However, though experiments can permit direct observation, incorrect operations and low-precision apparatuses will lead to errors in experimental results [15]. Additionally, the modeling and computational steps of numerical simulations are always time-costly and software-dependent [16,17]. Unlike the above methods, analytical solutions have been frequently used in recent years due to their ease of calculation [18,19]. For example, Peng et al. [20] considered the effects of diffusion, adsorption and degradation of organic contaminants on the performance of the CGCW and established a 2D analytical solution.

GMB defects are the main cause of GMB failure and will affect the performance of the CGCW. It is found that a GMB hole (even if it is smaller than 10 mm) will lead to a significant leakage [21]. The increase in the hole diameter can also cause a large leakage increase [22]. There are several empirical equations for the hole leakage calculation [23]. For example, Rowe et al. [24] established an empirical equation to predict leakages of different wrinkle heights and widths and tested it with landfills observed data in North America. Rowe and Fan [25] proposed new empirical equations to evaluate GMB hole leakage covered by saturated tailings based on experiments. However, all mentioned analytical studies on the performance of the CGCW didn't take into consideration the impact of GMB holes on contaminant transport. This will overestimate the service time and hydraulic performance of the CGCW [26]. Additionally, the field investigations and experiments show that the shapes of GMB holes are not always circular and water flow rates vary with GMB hole shapes [27,28]. For example, Sharma and Fang [29] found that the leakage of a triangular hole is 5% higher than that of a circular hole with the same area. There is no simple method to calculate the leakage of different hole shapes in the CGCW and aquifer system, currently. Thus, it is necessary to propose a new simple method to evaluate the performance of the CGCW under different hole shapes and sizes.

This paper aims to obtain empirical equations to predict leakages through the CGCWs using different hole shapes based on the numerical model. Additionally, an analytical solution is developed to evaluate the transient convection and diffusion of contaminants in the CGCW and aquifer system with adsorption. The key effects of the hole radius, hole shape, cut-off wall hydraulic coefficient and head loss on the performance of the CGCW are illustrated.

2. Materials and Methods

2.1. Numerical Model

A 3D numerical model consisting of a CGCW and aquifer system is established to evaluate the effects of GMB holes based on *COMSOL Multiphysics 6.0*. A 0.0015 m HDPE GMB is embedded into the SB cut-off wall (SBCW). The upstream SBCW, downstream SBCW and the aquifer thicknesses are assumed to be equal to 0.6 m, 0.6 m and 10 m, respectively. The cross-section of the model is a 1 m^2 square and the GMB hole is located in the center of the cross-section. The Transport of Diluted Species in Porous Media and Darcy's Law Interfaces of COMSOL are used to simulate leachate migration in the CGCW and aquifer system. The influences of GMB thickness (T_G), cut-off wall hydraulic conductivity (k_G), hole radius (r_G) and head loss (H_G) on leakages through the hole are investigated.

To obtain a simple method for predicting leakages for different shapes of holes, the Parametric Sweep option in COMSOL is used. Additionally, the empirical equation proposed in the study of Fan and Rowe [22] is used as a basis equation. In other words, the empirical equations for different shapes of holes all follow the form:

$$Q = ak_G H_G T_G^b r_G^{c\ln T+d} \quad (1)$$

where, a, b, c and d are all empirical coefficients and Q is the leakage.

2.2. Mathematical Model

A CGCW consisting of an upstream SBCW, an HDPE GMB and a downstream SBCW is installed to prevent the aquifer from being polluted by contaminants, as shown in

Figure 1. A one-dimensional model considering the effect of advection, hydrodynamic dispersion and adsorption is established to evaluate the performance of the CGCW. The thicknesses of the upstream SBCW, HDPE GMB, downstream SBCW and aquifer are denoted as L_1, L_2, L_3 and L_4, respectively. The following assumptions are made to develop the mathematical model:

(1) The SBCWs, GMB and aquifer are saturated, homogeneous and isotropic.
(2) The groundwater flows in a horizontal direction at a constant velocity.
(3) The thickness of the aquifer is large enough to ignore the effect of contaminant outflow.
(4) The adsorption of contaminants only occurs in SBCWs.

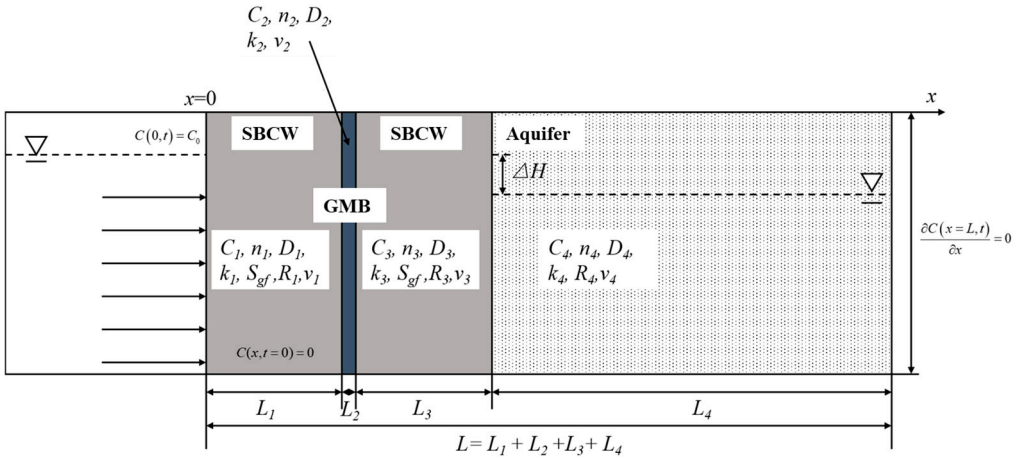

Figure 1. Mathematical model of contaminant transport in the CGCW and aquifer system.

The governing equations for contaminant transport in the CGCW and aquifer system can be given as follows [30]:

$$R_{di}\frac{\partial C_i}{\partial t} = D_i\frac{\partial^2 C_i}{\partial x^2} - v_i\frac{\partial C_i}{\partial x}(i = 1,\ 2,\ 3,\ 4) \tag{2}$$

where, i = 1, 2, 3, 4 refer to the upstream SBCW, HDPE GMB, downstream SBCW and aquifer; C_i is the contaminant concentration; x is the contaminant migration direction; D_i is the diffusion coefficient; R_{di} is the retardation factor; v_i is the average linear velocity of contaminants.

It should be noted that R_{d2} and R_{d4} are equal to 1 [31]. The retardation factors, diffusion coefficients and average linear velocities in the upstream SBCW and downstream SBCW are equal.

It is assumed that there is no contaminant in the system initially [18]:

$$C_i(x, t = 0) = 0 \tag{3}$$

The constant contaminant concentration inlet boundary is assumed at x = 0 [19]:

$$C_1(0, t) = C_0 \tag{4}$$

The outflow boundary is a semi-infinite boundary and can be expressed as [31]:

$$\frac{\partial C_4(L, t)}{\partial x} = 0 \tag{5}$$

The concentration and mass flux continuity conditions at the upstream SBCW and the GMB interface, the GMB and the downstream SBCW interface, the downstream SBCW and the aquifer interface can be expressed as [12,13]:

$$C_1(x,t)|_{x=L_1} = \left.\frac{C_2(x,t)}{S_{gf}}\right|_{x=L_1} \tag{6a}$$

$$D_1\left.\frac{\partial C_1(x,t)}{\partial x}\right|_{x=L_1} = S_{gf}D_2\left.\frac{\partial C_2(x,t)}{\partial x}\right|_{x=L_1} \tag{6b}$$

$$\left.\frac{C_2(x,t)}{S_{gf}}\right|_{x=L_1+L_2} = C_3(x,t)|_{x=L_1+L_2} \tag{6c}$$

$$S_{gf}D_2\left.\frac{\partial C_2(x,t)}{\partial z}\right|_{x=L_1+L_2} = D_3\left.\frac{\partial C_3(x,t)}{\partial z}\right|_{x=L_1+L_2} \tag{6d}$$

$$C_3(x,t)|_{x=L_1+L_2+L_3} = C_4(x,t)|_{x=L_1+L_2+L_3} \tag{6e}$$

$$D_3\left.\frac{\partial C_3(x,t)}{\partial x}\right|_{x=L_1+L_2+L_3} = D_4\left.\frac{\partial C_4(x,t)}{\partial x}\right|_{x=L_1+L_2+L_3} \tag{6f}$$

where, S_{gf} is the partition coefficient between the SBCW and the GMB.

The following parameters are introduced to simplify equations:

$$X_i = \frac{x_i}{L}T = \frac{D_1 t}{R_1 L^2}P_{ei} = \frac{v_i L}{D_i}\zeta_i = \frac{D_1 R_i}{R_1 D_i}f_i = \frac{D_{zi}}{L} \tag{7}$$

Equations (2)–(6) can be transformed into the following equations:

$$\zeta_i\frac{\partial C_i(X,T)}{\partial T} = \frac{\partial^2 C_i(X,T)}{\partial X^2} - P_{ei}\frac{\partial C_i(X,T)}{\partial T} \tag{8}$$

$$C(X,T=0) = 0 \tag{9a}$$

$$C(0,T) = C_0 \tag{9b}$$

$$\frac{\partial C(X=1,T)}{\partial X} = 0 \tag{9c}$$

$$C_1\left(X=\frac{L_1}{L},T\right) = \frac{C_2\left(X=\frac{L_1}{L},T\right)}{S_{gf}} \tag{9d}$$

$$f_1\frac{\partial C_1\left(X=\frac{L_1}{L},T\right)}{\partial X} = S_{gf}f_2\frac{\partial C_2(X,T)}{\partial X} \tag{9e}$$

$$\frac{C_2(X,T)}{S_{gf}} = C_3(X,T) \tag{9f}$$

$$S_{gf}f_2\frac{\partial C_2(X,T)}{\partial X} = f_3\frac{\partial C_3(X,T)}{\partial X} \tag{9g}$$

$$C_3(X,T) = C_4(X,T) \tag{9h}$$

$$f_3\frac{\partial C_3(X,T)}{\partial X} = f_4\frac{\partial C_4(X,T)}{\partial X} \tag{9i}$$

where, S_{gf} is the partition coefficient between the SBCW and the GMB.

The numerical Laplace inversion proposed by Abate et al. [32] is used to obtain the analytical solution:

$$f(t,M) = \frac{2}{5t}\sum_{k=0}^{M-1} Re\left(\gamma_k\overline{f\left(\frac{\delta_k}{t}\right)}\right) \tag{10}$$

and

$$\gamma_0 = \frac{1}{2}e^{\delta_0} \tag{11a}$$

$$\gamma_k = \left(1 + i\frac{k\pi}{M}\left(1 + \cot^2\left(\frac{k\pi}{M}\right) - i\cot\left(\frac{k\pi}{M}\right)\right)\right)e^{\delta_k}, 0 < k < M \tag{11b}$$

$$\delta_0 = \frac{2M}{5} \tag{11c}$$

$$\delta_k = \frac{2k\pi}{5}\left(\cot\left(\frac{k\pi}{M}\right) + i\right), 0 < k < M \tag{11d}$$

It should be noted that i is the imaginary number and M is assumed to be 64.

2.3. Parameter Analysis

Toluene (TOL) is chosen as the typical contaminant to investigate the effects of the hole radius, hole shape, cut-off wall hydraulic coefficient and head loss on the performance of the CGCW. According to the study by Giao [33], the concentrations of TOL in the polluted sites can be 10 mg/L. Additionally, the maximum allowable concentration for TOL behind the CGCW is assumed to be 1 mg/L. Thus, the relative breakthrough concentration for TOL is regarded as 0.1. All other parameters used are shown in Table 1. It should be noted that the GMB is embedded in the center of the cut-off wall. The shape of the GMB hole is assumed to be circular in Sections 4.2.1–4.2.3.

Table 1. Main parameters for the simulation.

		SBCW	GMB	Aquifer
Porosity		0.42 [31]	-	0.47 [31]
Hydraulic conductivity (m/s)		1.0×10^{-9} [34]	1.0×10^{-14} [34]	1.0×10^{-5} [34]
Thickness (m)		0.6 [12]	0.0015 [20]	10 [12]
Cross-sectional area (m^2)		1	1	1
Partition coefficient	MTBE	-	0.6 [35]	-
	TOL	-	100 [35]	-
Retardation factor	MTBE	1.5 [20]	-	1 [20]
	TOL	2.5 [20]	-	1 [20]
Diffusion coefficient (m^2/s)	MTBE	3.5×10^{-10} [21]	7.7×10^{-13} [21]	3.3×10^{-10} [21]
	TOL	3.8×10^{-10} [36]	3.8×10^{-13} [36]	4.1×10^{-10} [36]

3. Verification of the Analytical Solution

3.1. Compared with the Numerical Model

The 1D numerical model is established to verify the proposed analytical solution in this section. Darcy's Law and Transport of Diluted Species in Porous Media modulus are used to simulate the contaminant transport through CGCW and aquifer system. The thicknesses of the SBCW, GMB, and aquifer are assumed to be 0.6 m, 0.0015 m and 10 m [12,20]. The extra fine physics-controlled meshing sequences are invoked and 166 computational units are generated. Methyl tertiary butyl ether (MTBE) is considered as the contaminant in the source [33]. The parameters used in the calculation are all listed in Table 1. It should be noted that the leakage through the GMB is calculated to be 2.7×10^{-10} m/s in this section. It can be concluded from Figure 2 that the results obtained from the analytical solution are in agreement with those from the numerical simulations. The differences between the results predicted by the proposed analytical solution and the numerical model for t = 25 and 50 years are only 0.1% and 0.12%, respectively. This indicates that the analytical solution can accurately predict contaminants transport through the CGCW and aquifer system.

Additionally, the CGCW can effectively block the water flow and decrease the contaminant concentration in the groundwater. For example, the contaminant concentrations at x = 0.6 and 0.6015 are 0.73 and 0.31 when t = 25 years, respectively. The main reason for this phenomenon is that the diffusion coefficients (7.7×10^{-13} m^2/s) and partition coefficients (0.6) in GMB for MTBE are small. GMB can effectively impede the transport of MTBE. This will lead to a huge contaminant concentration mutation between two sides of GMB [30].

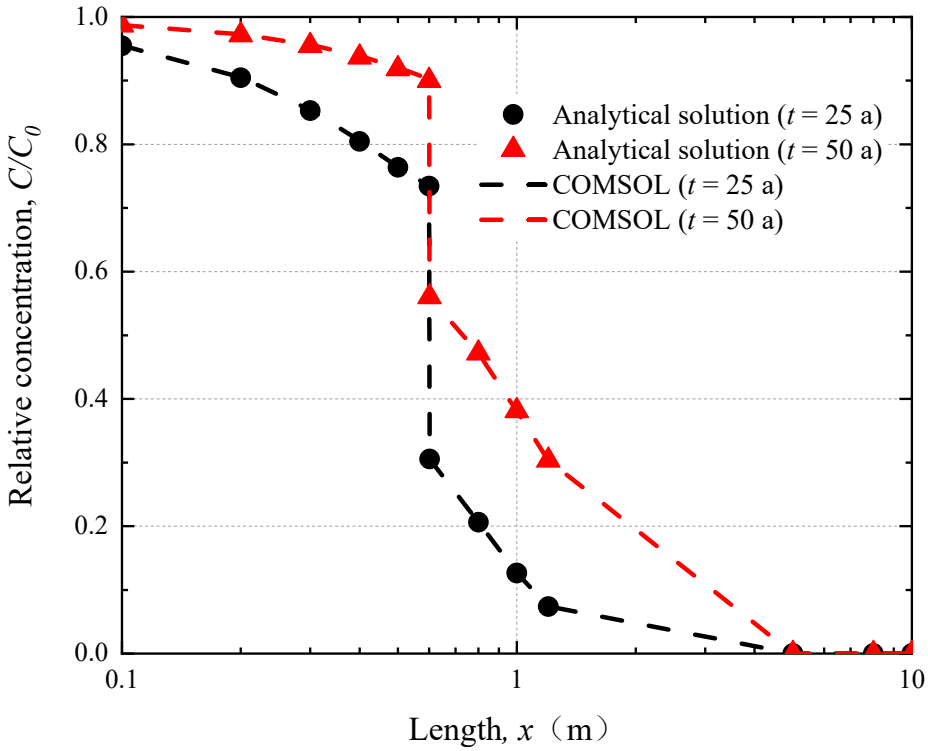

Figure 2. Comparison with the results predicted by COMSOL.

3.2. Compared with the Existing Analytical Model

A pure diffusion analytical model proposed by Peng et al. [30] is selected to verify the proposed solution. The values of parameters used for comparison are the same as those in Section 3.1. The breakthrough curves of the CGCW under different leakages are shown in Figure 3. It can be concluded that the difference between the results predicted by the pure diffusion model and the proposed model is only 1.01% when there is no leakage (v_2 = 0). This demonstrates the accuracy of the proposed solution. Additionally, it can be found that the leakage can pose significantly effects on the CGCW performance. For example, the contaminant concentrations for $v_2 = 10^{-9}$ m/s can be 7.43 and 1.79 times larger than that for $v_2 = 10^{-10}$ m/s and $v_2 = 5 \times 10^{-10}$ m/s when t = 50 years, respectively. It indicates that the effects of leakage caused by the GMB holes should be taken into consideration. Additionally, the proposed solution can offer more accurate suggestions for the design of the CGCW.

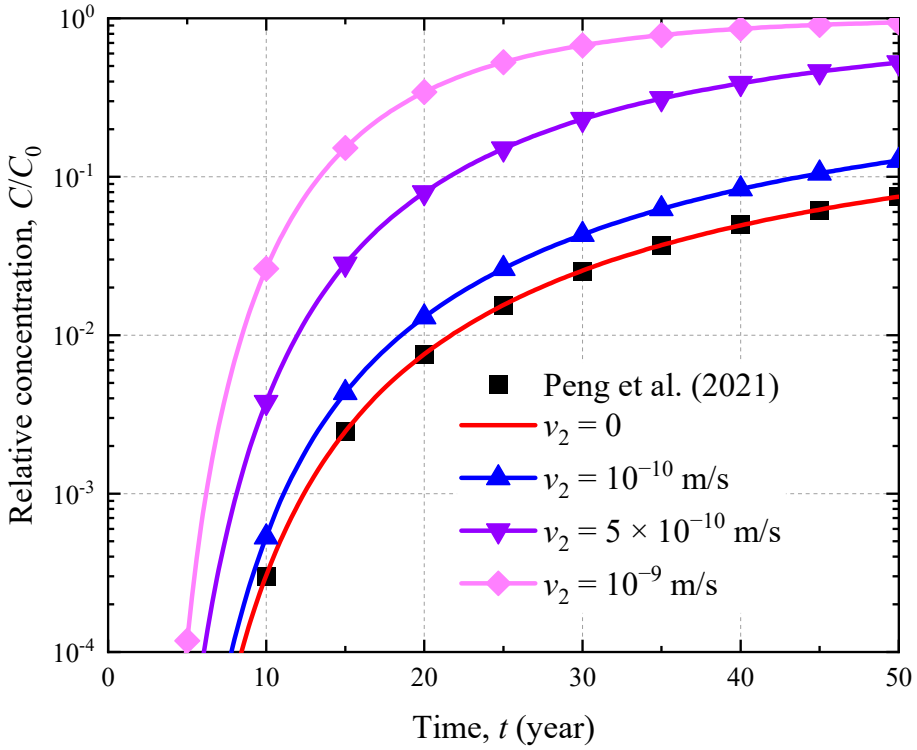

Figure 3. Comparison with the existing analytical model by Peng et al. (2021) [30].

4. Results and Discussion

4.1. Leakage Prediction

4.1.1. Influence of GMB Thickness, Head Loss, and Cut-Off Wall Hydraulic Conductivity on Leakage

Increasing the GMB thickness and decreasing the head loss and cut-off wall hydraulic conductivity can decrease the leakage (Figure 4). For example, the leakage for T_G = 0.002 m is 1.52 × 10^{-10} m^3/s while it for T_G = 0.001 m is 1.85 × 10^{-10} m^3/s when k_G = 1 × 10^{-9} m/s, r_G = 0.005 m, and H_G = 10 m. The values of the leakage and head loss are linearly related. For example, increasing the H_G from 1 m to 10 m leads to a 10-time increase in the leakage. Experiments conducted by Rowe and Fan [25] have also proved this conclusion. Additionally, it can be concluded that changing the T_G has an insignificant influence on the leakage when the k_G is small. For example, the leakage for T_G = 0.002 m is 1.22 times smaller than that for T_G = 0.001 m when k_G = 1 × 10^{-9} m/s, r_G = 0.005 m. However, the difference decreases to 1.02 times when k_G = 1 × 10^{-11} m/s. This is mainly because the SBCWs are the dominant parts to prevent leakage, though increasing the GMB thickness can lead to a decrease in the hydraulic gradient [25].

4.1.2. Influence of the Hole Radius on Leakage

Increasing the hole radius leads to an increase in the leakage (Figure 5). Additionally, it can be concluded based on the results that there is no linear relationship between the leakage and GMB radius. For example, the leakage for r_G = 0.05 m is 5.8 and 3.1 times larger than that for r_G = 0.005 and 0.025 m, respectively. However, according to the study of Fan and Rowe [25], the increase in the leakage is slightly larger than linearly with the hole radius. The main reason for this difference is that Fan and Rowe [25] considered the influence of the GMB hole when covered by tailings rather than embedded in the cut-off wall. The cut-off wall has low permeability and can prevent leakage. Thus, the effects of the geometric properties of the hole on the leakage will be weakened. Moreover, an interesting conclusion is found that the change of the leakage caused by the change of the cut-off wall hydraulic coefficient is related to the hole radius. For example, the leakages for r_G = 0.005, 0.025 and 0.05 m when k_G = 1 × 10^{-11} m/s are 2.4, 12.3 and 21.1 times lower than those

when $k_G = 1 \times 10^{-9}$ m/s. The increases in leakages are approximately linearly with the hole radiuses.

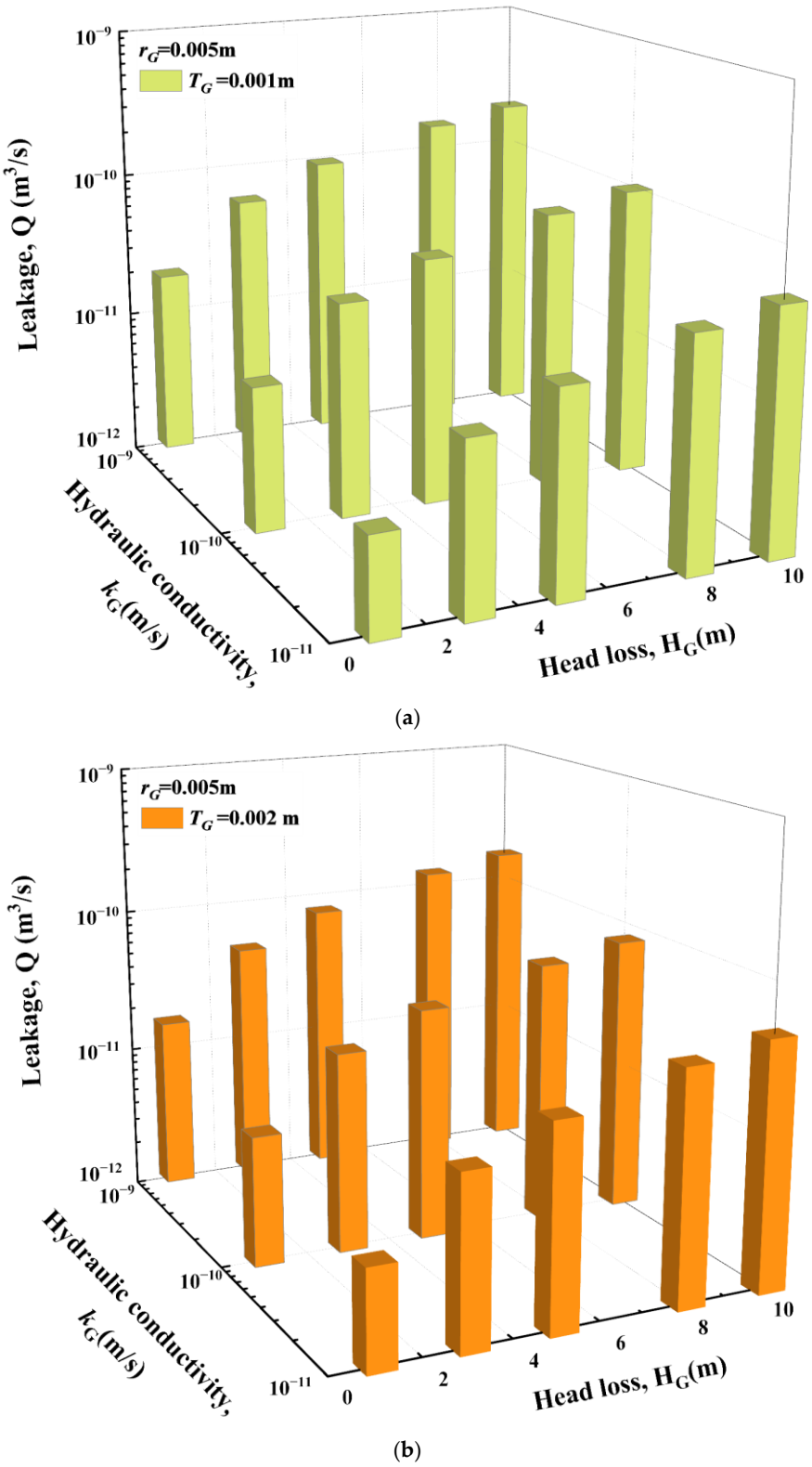

Figure 4. Leakages for different hydraulic conductivities and head losses when (**a**) T_G = 0.001 m and (**b**) T_G = 0.002 m.

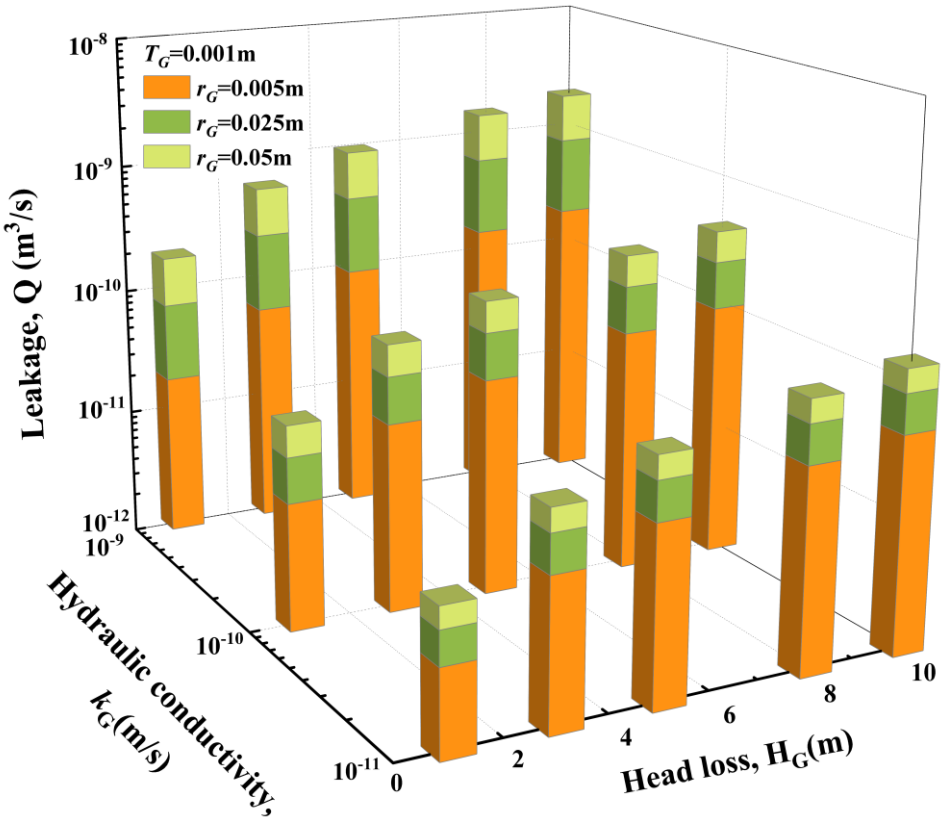

Figure 5. Leakages for different hydraulic conductivities and head losses with different GMB thicknesses.

4.1.3. Influence of the Hole Shape on Leakage

The effects of different hole shapes such as circular, triangular, rhombic, square, and rectangular on the leakage are investigated. The dimensional drawing of the designed GMB holes are shown in Figure 6. To avoid the influence of the different hole areas on the leakage, hole areas of all shapes are assumed to be 1960 mm^2. The cut-off wall hydraulic coefficient, head loss and GMB thickness are assumed to be 1×10^{-9} m/s, 1 m and 0.0015 m, respectively [31]. It can be calculated that the leakage in the circular hole is 5.3×10^{-11} m^3/s while leakages for other hole shapes are in the range of 1.28×10^{-10} m^3/s–1.32×10^{-10} m^3/s. This is mainly because the shape factor for the circular hole is 1.15–1.3 times lower than that for other shapes of holes with the same area [25]. It leads to the appearance of a lower leakage in the circular hole. Similar conclusions have also reported by Xia et al. [37]. They found that compared with other hole shapes, the stress distribution around the circular hole is more uniform. This can help minimize tearing or failure of the GMB caused by the stress concentration at any single point.

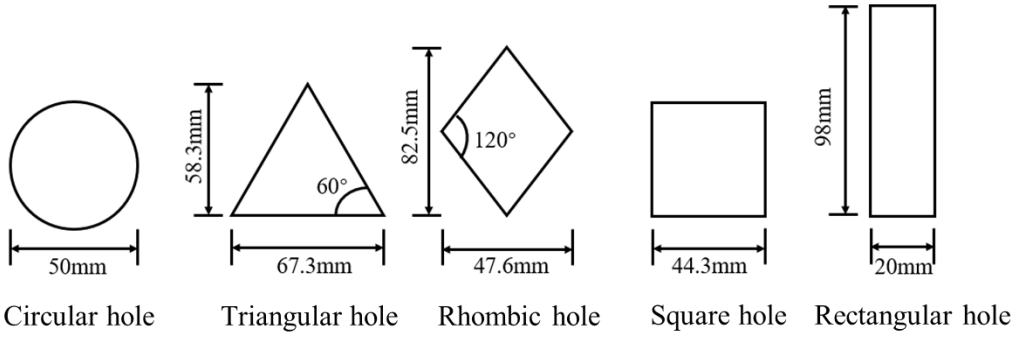

Figure 6. Dimensional drawing of different GMB hole shapes.

4.1.4. Empirical Equations for the Prediction of the Leakages

2500 conditions with r_G in the range of 0.005–0.05 m, T_G in the range of 0.001–0.0025 m, k_G in the range of 1×10^{-9} m/s^{-1} $\times$ 10^{-11} m/s and H_G in the range of 0.6 m–10 m are analyzed. Empirical equations to predict leakages for different shapes of holes are all shown in Table 2. It should be noted that in the empirical equations, the parameter r_G represents the radius of circular holes with the same area for different hole shapes. It can be concluded that R^2 for all equations are larger than 0.91. It indicates that the proposed empirical equations are suitable for evaluating the leakage in a CGCW and aquifer system.

Table 2. Empirical equations to predict leakages for different shapes of holes.

Hole Shape	Empirical Equation	R^2
Circular	$Q = 0.2769 k_G H_G T_G^{0.0462} r_G^{0.0971 \ln T_G + 0.8235}$	0.99
Triangular	$Q = 0.9572 k_G H_G T_G^{0.4854} r_G^{0.08 \ln T_G + 0.1419}$	0.91
Rhombic	$Q = 0.1966 k_G H_G T_G^{0.2511} r_G^{0.616 \ln T_G + 0.4733}$	0.93
Square	$Q = 0.3804 k_G H_G T_G^{0.5678} r_G^{0.0759 \ln T_G + 0.054}$	0.91
Rectangular	$Q = 0.7094 k_G H_G T_G^{0.7547} r_G^{0.276 \ln T_G + 0.6797}$	0.92

4.2. CGCW Performance Analysis

4.2.1. Influence of the Hole Radius

The influence of the hole radius (r_G) on the breakthrough curve of the CGCW is shown in Figure 7. The H_G is assumed to be 3.0 m. It can be concluded that increasing r_G can lead to a decrease in the breakthrough time. However, this effect can be insignificant when k_G is small (e.g., <10^{-10} m/s). For example, the breakthrough times for r_G = 0.005 m and 0.05 m are 47.3 and 48.1 years when k_G = 10^{-10} m/s, respectively. Additionally, the breakthrough time for r_G = 0.005 m is 5 years longer than that for r_G = 0.05 m when k_G = 10^{-9} m/s. The main reason is that the impermeability of the CGCW is good when k_G is small (as mentioned in Section 3.2). This will weaken the impacts of the hole geometric properties on the leakage. Moreover, it can also be observed from the empirical equations in Table 2 that leakage is directly proportional to both k_G and $r_G{}^{0.192}$, respectively. The influence of k_G is more significant than that of r_G. In other words, reducing k_G can minimize the negative influence of GMB holes on the service time of the CGCWs. Therefore, it is essential to use the cut-off wall materials with lower hydraulic conductivities in the actual projects.

4.2.2. Influence of the Hole Shape

The influence of the hole shape on the breakthrough curve of the CGCW is shown in Figure 8. Two different hole shapes including circular and rectangular holes are analyzed. The H_G, r_G and T_G are assumed to be 3 m, 0.05 m and 0.0015 m, respectively. Compared with other hole shapes, the performance of the CGCW is better when the GMB holes are circular. For example, the breakthrough time for a circular hole is 1.1 times larger than that for a rectangular hole when k_G = 10^{-9} m/s. It is mainly because the leakage through a circular hole is lower than that through other shapes of holes as the shape factor for the circular hole is lowest. Additionally, it can be found that the influence of the hole radius and shape are similar. The same trend that the parameter impacts will be weakened when the impermeability of the CGCW is good. For example, the breakthrough time for the circular hole is only 0.9 years longer than that for the rectangular hole when k_G = 10^{-10} m/s.

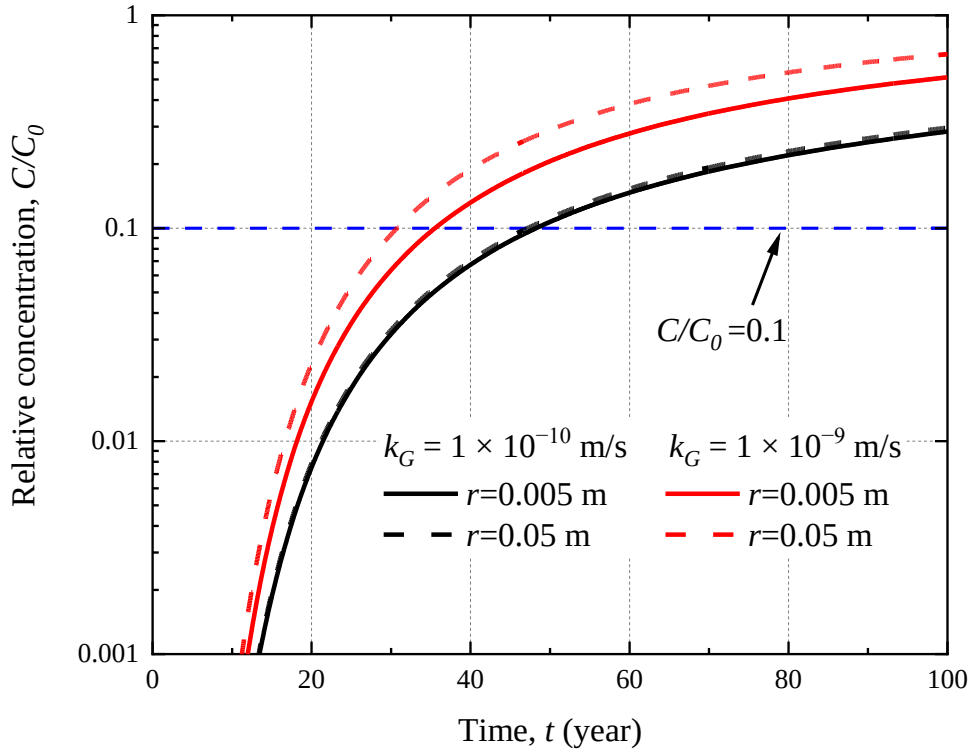

Figure 7. Influence of the hole radius on the breakthrough curve.

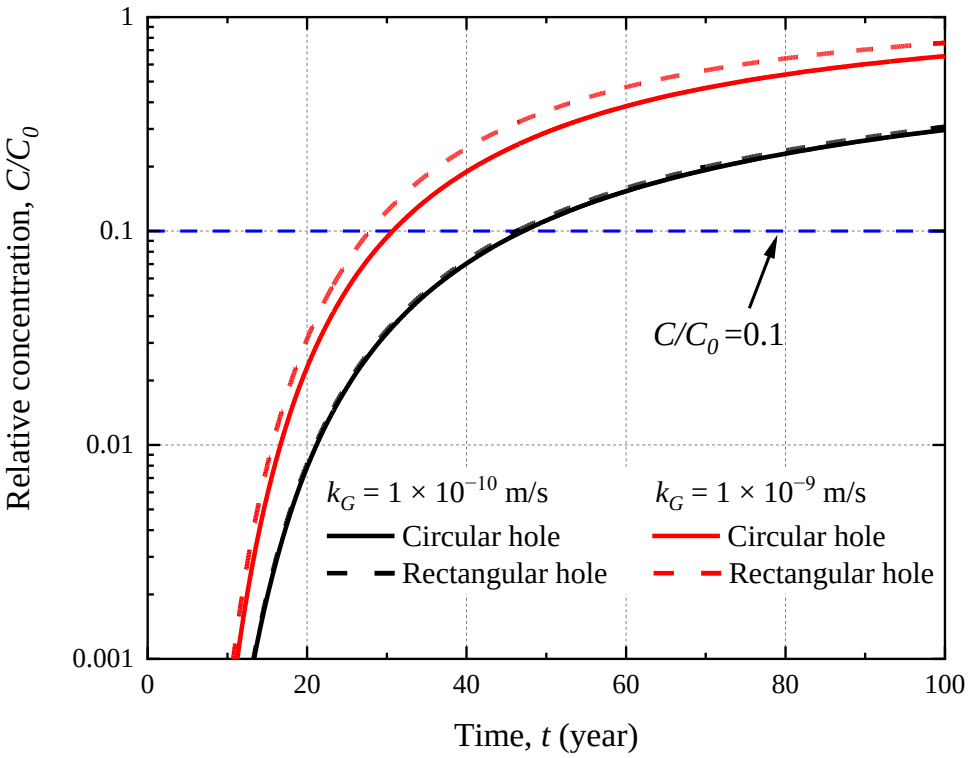

Figure 8. Influence of the hole shape on the breakthrough curve.

4.2.3. Influence of the Cut-Off Wall Hydraulic Coefficient

The influence of the cut-off wall hydraulic coefficient (k_G) on the breakthrough curve of the CGCW is shown in Figure 9. The H_G, r_G and T_G are assumed to be 3.0 m, 0.05 m and 0.0015 m, respectively. Increasing the k_G can result in a worse performance of the CGCW. For example, the breakthrough time for $k_G = 10^{-10}$ m/s is 1.3 and 1.5 times larger than that

for $k_G = 5 \times 10^{-10}$ m/s and 1×10^{-9} m/s, respectively. This is mainly because decreasing k_G can significantly decrease the leakage. This has also been mentioned in Section 4.1. Additionally, it can be concluded that k_G has little effect on the CGCW performance when it is small (e.g., $<10^{-10}$ m/s). The breakthrough curves of $k_G = 10^{-10}$ m/s and 10^{-11} m/s are almost coincident. The breakthrough time for $k_G = 10^{-11}$ m/s is only 1.06 times larger than that for $k_G = 10^{-10}$ m/s. The dispersion can be the dominant mechanism for contaminant transport as the Peclet number in the cut-off wall is lower than 1 (e.g., <0.26) when $k_G < 10^{-10}$ m/s. Thus, there is a threshold for k_G in the CGCW (e.g., 10^{-10} m/s) that can not only satisfy economic and safety needs. In other words, decreasing k_G cannot help much to the CGCW performance when it is lower than the threshold. It can be very important to find the threshold in the design of the CGCW.

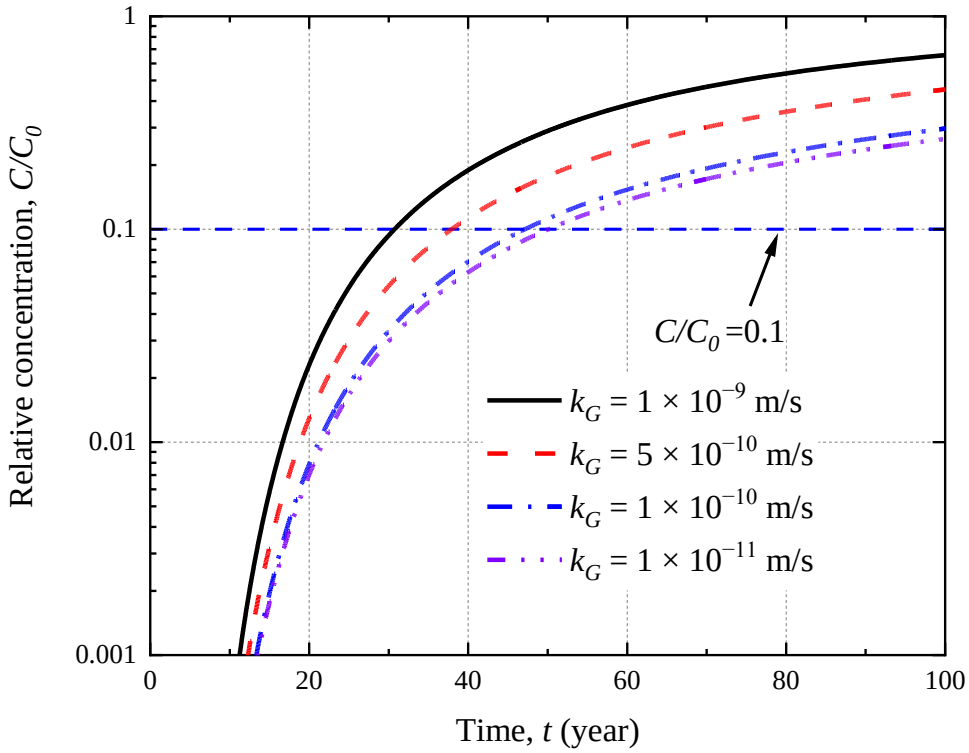

Figure 9. Influence of the cut-off wall hydraulic conductivity on the breakthrough curve.

4.2.4. Influence of the Head Loss

The influence of the head loss (H_G) on the breakthrough curve of the CGCW is shown in Figure 10. The r_G, T_G and are assumed to be 0.05 m and 0.0015 m, respectively. Increasing H_G can lead to a decrease in the breakthrough time. For example, the breakthrough time for $H_G = 0.3$ m is 30 years longer than that for $H_G = 10$ m when $k_G = 10^{-9}$ m/s. The main reason is that the contaminant transport in the CGCW can be accelerated with the increase of H_G. More contaminants can break through the barrier and migrate to the groundwater. Thus, the methods that can control the head loss (e.g., a pumping well) should be taken to improve the performance of the CGCW. Additionally, it can be concluded that the effect of H_G can be weakened when the impermeability of the barrier wall is relatively good (e.g., $k_G = 10^{-10}$ m/s). For example, although H_G increases by 33-fold (from 0.3 m to 10 m), the breakthrough time of the CGCW is only 1.2 times larger than before when $k_G = 10^{-10}$ m/s. It can also be demonstrated from the empirical equation for circular holes in Table 2 that even if the head loss is large (e.g., 10 m), the leakage is lower than 1.2×10^{-10} m^3/s when $k_G = 10^{-10}$ m/s.

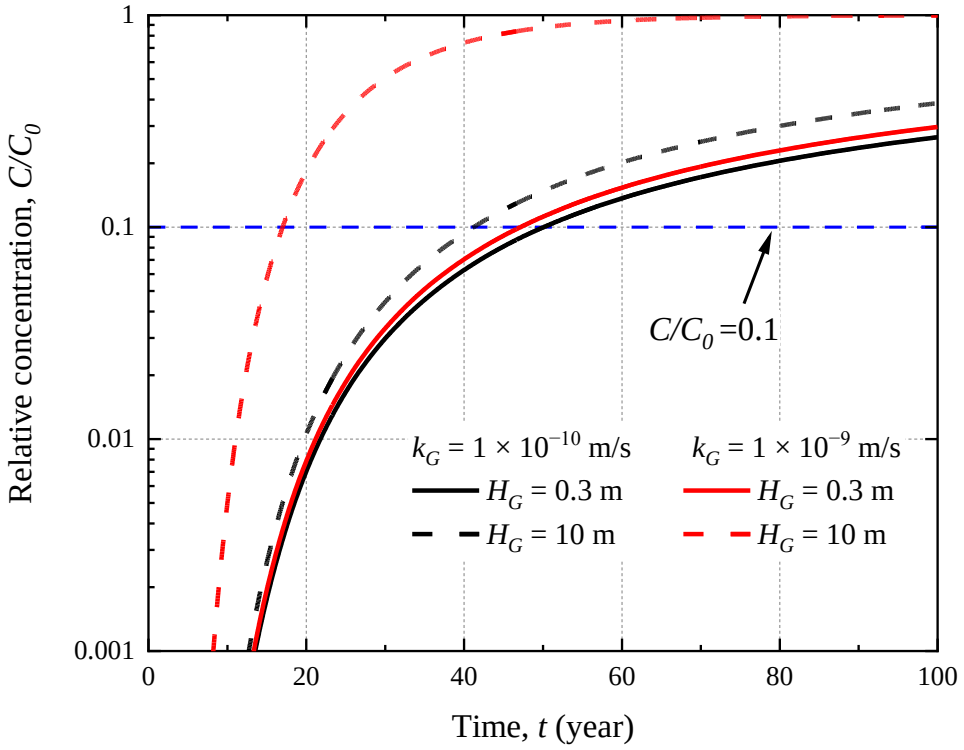

Figure 10. Influence of the head loss on the breakthrough curve.

5. Limitation

The proposed analytical model is not without limitation. One of the major limitations is that the heterogeneity of CGCW cannot be taken into consideration since the model is one-dimensional. It has been proved that the compaction and uneven density of the CGCW materials generated during the production and installation can significantly affect the porosity and hydraulic conductivity at different locations in the wall [38]. The actual contaminant concentrations behind the CGCW can be larger or lower than the results predicted by the model. Another limitation is that the parameters of the SBCW are assumed not to change with time. However, the materials of the cut-off wall can be easily affected by contaminants during the service life [39]. This can result in a gradual increase in the hydraulic conductivity. Further numerical simulations are recommended to investigate the effects of the heterogeneity and parameter time-variation on the CGCW performance.

The empirical equations proposed in this manuscript also have limitations. The parametric sweep feature is used to simulate the leakage of the GMB holes under different situations. However, the effects of the parameter uncertainty on the leakage and CGCW performance cannot be taken into consideration. It has been proved that the analysis of parameter uncertainty can offer significant helps in the engineering design since it can help in further identifying critical factors that influence the leakage behavior [31]. Uncertainty quantification feature of COMSOL is expected to be used in the future study to quantify the uncertainty in model outcomes caused by uncertainties in input parameters.

6. Conclusions

This paper proposes the empirical equations and analytical model to evaluate the performance of the CGCW while considering the effects of GMB holes. The accuracy of the established equations and analytical solution is confirmed by the numerical models. The key effects of the GMB thickness, head loss, cut-off wall hydraulic conductivity, hole radius and shape on the leakage and CGCW performance are investigated.

(1) The proposed solution can offer more accurate suggestions for the design of the CGCW than the pure diffusion model, especially when the leakage is large (e.g.,

>10^{-10} m/s). For example, the contaminant concentrations for $v_2 = 10^{-9}$ m/s can be 7.43 and 1.79 times larger than that for $v_2 = 10^{-10}$ m/s and $v_2 = 5 \times 10^{-10}$ m/s when $t = 50$ years, respectively.

(2) The values of the leakage and head loss are linearly related. For example, increasing the head loss from 1 m to 10 m leads to a 10-time increase in the leakage. Additionally, changing the GMB thickness has an insignificant influence on the leakage when the k_G is small. Thus, the pumping method is suggested to be used to control the head loss and improve the CGCW performance in practical engineering.

(3) Various hole shapes can lead to different performances of the CGCW. Additionally, the performance of the CGCW is better when the GMB hole is circular. For example, the breakthrough time for the circular hole is 1.1 times larger than that for the rectangular hole when $k_G = 10^{-9}$ m/s. This is mainly because the leakage through the circular hole is low as the shape factor for the circular hole is 1.15–1.3 times lower than that for other shapes of holes.

(4) The influences of the hole radius, shape and head loss on the breakthrough curve of the CGCW seem to be more significant when hydraulic conductivity is large. For example, although the head loss increases by 33-fold (from 0.3 m to 10 m), the breakthrough time of the CGCW is only 1.2 times larger than before when $k_G = 10^{-10}$ m/s. Thus, the hydraulic conductivity of the cut-off wall is suggested to be controlled lower than 10^{-9} m/s.

Author Contributions: L.R.: Conceptualization, Methodology, Validation, Visualization, Writing—original draft, Writing—review & editing. G.W.: Validation, Investigation, Writing—review & editing. H.D.: Conceptualization, Project administration, Resources, Supervision, Writing—original draft, Writing—review & editing. H.X.: Funding acquisition, Investigation, Writing—review & editing. All authors have read and agreed to the published version of the manuscript.

Funding: The financial supports from the National Key R&D research and development Program of China (Grant No. 2023YFC3709602), National Natural Science Foundation of China (Grant Nos. 52278375, 41931289, and 41977223), and Zhejiang Provincial Natural Science Foundation (Gran No. LR20E080002) are greatly acknowledged.

Institutional Review Board Statement: Not applicable.

Informed Consent Statement: Informed consent was obtained from all subjects involved in the study.

Data Availability Statement: Data are available from the authors upon reasonable request.

Conflicts of Interest: Authors Guijun Wan, Haijian Xie and Hao Ding were employed by the company The Architectural Design and Research Institute of Zhejiang University Co., Ltd.; the remaining authors declare that the research was conducted in the absence of any commercial or financial relationships that could be construed as a potential conflict of interest.

References

1. Rao, N.S.; Dinakar, A.; Sun, L. Estimation of groundwater pollution levels and specific ionic sources in the groundwater, using a comprehensive approach of geochemical ratios, pollution index of groundwater, unmix model and land use/land cover–A case study. *J. Contam. Hydrol.* **2022**, *248*, 103990.
2. Li, F.; Wu, J.; Xu, F.; Yang, Y.; Du, Q. Determination of the spatial correlation characteristics for selected groundwater pollutants using the geographically weighted regression model: A case study in Weinan, Northwest China. *Hum. Ecol. Risk Assess. Int. J.* **2022**, *29*, 471–493. [CrossRef]
3. Wu, Y.-X.; Shen, S.-L.; Yin, Z.-Y.; Xu, Y.-S. Characteristics of groundwater seepage with cut-off wall in gravel aquifer. II: Numerical analysis. *Can. Geotech. J.* **2015**, *52*, 1539–1549. [CrossRef]
4. Sun, W.; Zhang, G.; Zhang, Z. Damage analysis of the cut-off wall in a landslide dam based on centrifuge and numerical modeling. *Comput. Geotech.* **2021**, *130*, 103936. [CrossRef]
5. Malusis, M.A.; Yeom, S.; Evans, J.C. Hydraulic conductivity of model soil–bentonite backfills subjected to wet–dry cycling. *Can. Geotech. J.* **2011**, *48*, 1198–1211. [CrossRef]
6. Evans, J.C. Hydraulic conductivity of vertical cutoff walls. *ASTM Spec. Tech. Publ.* **1994**, *1142*, 79.
7. Hinchberger, S.; Weck, J.; Newson, T. Mechanical and hydraulic characterization of plastic concrete for seepage cut-off walls. *Can. Geotech. J.* **2010**, *47*, 461–471. [CrossRef]

8. Bouazza, A.; Zornberg, J.G.; Adam, D. Geosynthetics in waste containment facilities: Recent advances. In *State-of-the-Art Keynote Paper, Proceedings of the Seventh International Conference on Geosynthetics, Nice, France, 22–27 September 2002*; A.A. Balkema: Cape Town, South Africa, 2002; Volume 2, pp. 445–510.
9. Qian, X.; Zheng, Z.; Guo, Z.; Qi, C.; Liu, L.; Liu, Y.; Zhen, S.; Ding, S.; Jin, J.; Wang, Y.; et al. Applications of geomembrane cutoff walls in remediation of contaminated sites. In Proceedings of the 8th International Congress on Environmental Geotechnics Volume 2: Towards a Sustainable Geoenvironment 8th, Hangzhou, China, 28 October–1 November 2018; Springer: Singapore, 2019; pp. 335–342.
10. Daniel, D.E.; Koerner, R.M. On the use of geomembranes in vertical barriers. In *Advances in Transportation and Geoenvironmental Systems Using Geosynthetics*; ASCE: Denver, CO, USA, 2000; pp. 81–93. [CrossRef]
11. Brandl, H. Vertical barriers for municipal and hazardous waste containment. In *Developments in Geotechnical Engineering: From Harvard to New Delhi 1936–1994*; CRC Press: Boca Raton, FL, USA, 2021; pp. 301–334.
12. Peng, C.H.; Feng, S.J.; Chen, H.X.; Luo, C.H.; Ding, X.H. Migration of organic contaminants in composite geomembrane cut-off wall considering groundwater seepage. *Chin. J. Geotech. Eng.* **2021**, *43*, 2055–2063.
13. Xu, H.; Sun, T.; Liu, S.; Zhang, N.; Wu, S.; Jiang, P.; Zhou, A. Study on the performance of sealing slurry at the bottom of geomembrane composite vertical cut off walls. *Process Saf. Environ. Prot.* **2023**, *180*, 945–958. [CrossRef]
14. Wang, M.; Fu, X.; Jiang, Z.; Che, C.; Jiang, N.; Du, Y. Swelling Behavior and Flow Rates of a Novel Hydrophilic Gasket Used in Composite Geomembrane Vertical Cutoff Walls and Infrastructures Exposed to Contaminated Groundwater. *Buildings* **2022**, *12*, 2207. [CrossRef]
15. Dai, G.; Zhu, J.; Song, Y.; Li, S.; Shi, G. Experimental study on the deformation of a cut-off wall in a landfill. *KSCE J. Civ. Eng.* **2020**, *24*, 1439–1447. [CrossRef]
16. Soini, E.J.; Rissanen, T.; Tiihonen, J.; Hodgins, S.; Eronen, M.; Ryynänen, O.-P. Predicting forensic admission among the mentally ill in a multinational setting: A Bayesian modelling approach. *Data Knowl. Eng.* **2009**, *68*, 1427–1440. [CrossRef]
17. Tamm, C.; Perfetto, S. Design and optimization of mechatronic systems using a holistic and parametric simulation approach. *IFAC-PapersOnLine* **2019**, *52*, 271–276. [CrossRef]
18. Xie, H.; Wu, J.; Thomas, H.R.; Cai, P.; Yan, H.; Chen, Y. An analytical model for contaminant transport in landfill liner with fluctuating leachate head. *Int. J. Numer. Anal. Methods Géoméch.* **2022**, *47*, 482–494. [CrossRef]
19. Yan, H.; Xie, H.; Rajabi, H.; Gu, X.; Chen, Y. Analytical solution for one-dimensional steady-state VOCs diffusion in simplified capillary cover systems. *Int. J. Numer. Anal. Methods Geomech.* **2023**, *47*, 2304–2321. [CrossRef]
20. Peng, C.-H.; Feng, S.-J.; Zheng, Q.-T.; Ding, X.-H.; Chen, Z.-L.; Chen, H.-X. A two-dimensional analytical solution for organic contaminant diffusion through a composite geomembrane cut-off wall and an aquifer. *Comput. Geotech.* **2019**, *119*, 103361. [CrossRef]
21. Abdel Razek, A.Y.; Rowe, R.K. Interface transmissivity of conventional and multicomponent GCLs for three permeants. *Geotext. Geomembr.* **2019**, *47*, 60–74. [CrossRef]
22. Fan, J.; Rowe, R.K. Seepage through a circular geomembrane hole when covered by fine-grained tailings under filter incompatible conditions. *Can. Geotech. J.* **2022**, *59*, 410–423. [CrossRef]
23. Li, Y.-C.; Yao, S.-Y.; Chen, C.; Chen, Y.-M.; Chen, G.-N.; Zhang, R.-H. A solution for calculating the leakage rate through GMB/CCL composite liners with long defects. *Comput. Geotech.* **2023**, *163*, 105770. [CrossRef]
24. Rowe, R.K.; Chappel, M.J.; Brachman, R.W.I.; Take, W.A. Field study of wrinkles in a geomembrane at a composite liner test site. *Can. Geotech. J.* **2012**, *49*, 1196–1211. [CrossRef]
25. Rowe, R.K.; Fan, J. Effect of geomembrane hole geometry on leakage overlain by saturated tailings. *Geotext. Geomembr.* **2021**, *49*, 1506–1518. [CrossRef]
26. Touze-Foltz, N.; Xie, H.; Stoltz, G. Performance issues of barrier systems for landfills: A review. *Geotext. Geomembr.* **2021**, *49*, 475–488. [CrossRef]
27. Rowe, R.K.; Brachman, R.W.I.; Irfan, H.; Smith, M.E.; Thiel, R. Effect of underliner on geomembrane strains in heap leach applications. *Geotext. Geomembr.* **2013**, *40*, 37–47. [CrossRef]
28. Gilson-Beck, A. Controlling leakage through installed geomembranes using electrical leak location. *Geotext. Geomembr.* **2019**, *47*, 697–710. [CrossRef]
29. Sharma, P.; Fang, T. Breakup of liquid jets from non-circular orifices. *Exp. Fluids* **2014**, *55*, 1666. [CrossRef]
30. Peng, C.-H.; Feng, S.-J.; Chen, H.-X.; Ding, X.-H.; Yang, C.-B. An analytical model for one-dimensional diffusion of degradable contaminant through a composite geomembrane cut-off wall. *J. Contam. Hydrol.* **2021**, *242*, 103845. [CrossRef]
31. Xie, H.; Shi, Y.; Yan, H.; Bouazza, A.; Zhu, X.; Wang, A. Analytical model for organic contaminant transport in a cut-off wall and aquifer dual-domain system considering barrier arrangements. *J. Contam. Hydrol.* **2023**, *259*, 104259. [CrossRef]
32. Abate, J.; Whitt, W. A unified framework for numerically inverting Laplace transforms. *Inf. J. Comput.* **2006**, *18*, 408–421. [CrossRef]
33. Giao, N.T. Potential health risk assessment for the occurrence of heavy metals in rice field influenced by landfill activity in Can Tho City, Vietnam. *Int. J. Environ. Agric. Biotechnol.* **2020**, *5*, 928–935. [CrossRef]
34. Wang, Y.; Chen, Y.; Xie, H.; Zhang, C.; Zhan, L. Lead adsorption and transport in loess-amended soil-bentonite cut-off wall. *Eng. Geol.* **2016**, *215*, 69–80. [CrossRef]

35. Hong, C.S.; Shackelford, C.D. Long-term column testing of zeolite-amended backfills. I: Testing methodology and chemical compatibility. *J. Geotech. Geoenviron. Eng.* **2017**, *143*, 04017050. [CrossRef]
36. Thornton, S.; Nicholls, H.; Rolfe, S.; Mallinson, H.; Spence, M. Biodegradation and fate of ethyl tert-butyl ether (ETBE) in soil and groundwater: A review. J. Hazard. Mater. 2020, 391, 122046Chen, Y.; Wang, Y.; Xie, H. Breakthrough time-based design of landfill composite liners. *Geotext. Geomembr.* **2015**, *43*, 196–206. [CrossRef]
37. Xia, Z.; Jiang, N.; Yang, H.; Han, L.; Pan, H.; Zhao, Z.; Feng, Q. Effect of multiple hole distribution and shape based on particle flow on rocklike failure characteristics and mechanical behavior. *Adv. Civ. Eng.* **2020**, *2020*, 8822225. [CrossRef]
38. Keramatikerman, M.; Chegenizadeh, A.; Nikraz, H. An investigation into effect of sawdust treatment on permeability and compressibility of soil-bentonite slurry cut-off wall. *J. Clean. Prod.* **2017**, *162*, 1–6. [CrossRef]
39. Joshi, K.; Kechavarzi, C.; Sutherland, K.; Ng, M.Y.A.; Soga, K.; Tedd, P. Laboratory and in situ tests for long-term hydraulic conductivity of a cement-bentonite cutoff wall. *J. Geotech. Geoenviron. Eng.* **2010**, *136*, 562–572. [CrossRef]